The Nuclear Equation of State: a Tool to Constrain In-Medium Hadronic Interactions*

F. Sammarruca[1] and P. G. Krastev[2]

[1] Physics Department, University of Idaho, Moscow, ID 83844-0903, U.S.A.
[2] Physics Department, Texas A&M University – Commerce, Commerce, TX 75429-3011, U.S.A.

Abstract. Recently we have been concerned with the properties of the nuclear equation of state (EOS), a relation between thermodynamic variables characterizing a medium. At zero temperature, such relation can be expressed in terms of energy (or pressure) as a function of density. Mechanisms such as isospin and/or spin asymmetry can have a dramatic impact on the equation of state. After briefly reviewing our previous work concerning the isospin asymmetries of the EOS, we will concentrate on our most recent results and their relevance towards a better understanding of the nuclear force in exotic matter. The approach we take is microscopic and relativistic. The calculated EOS properties are derived self-consistently from realistic nucleon-nucleon interactions. This makes it possible to understand the predictions in terms of specific features of the nuclear force model.

1 Introduction

Microscopic studies of nuclear matter under extreme conditions (for instance, extreme values of the neutron-to-proton ratio) are of great contemporary interest because of their relation to future experimental facilities. Although some delay may be expected, the planned Rare Isotope Accelerator (RIA) is still a high priority for major new construction in nuclear physics. Thanks to unprecedented beam fragmentation techniques, with RIA it will be possible to change the neutron-to-proton ratio in the colliding nuclei over a wide range. How the properties of nuclear systems depend on this ratio has been a central point of our recent work.

Furthermore, experiments with radioactive beams have made it possible to explore the still largely unknown regions of neutron or proton rich nuclei, including the so-called "halo" structures (identified by large spacial extension and increased interaction cross section as compared to their stable isotopes). Understanding the properties of these highly "exotic" nuclei require the knowledge of the nuclear force through the unusual topologies encountered near the drip lines (that is, systems with extreme neutron-to-proton ratios).

Motivated by all of the above arguments, in the past few years our efforts have been aimed at exploring nuclear interactions in neutron-rich matter through a broad spectrum of applications. These include:

* Support from the U.S. Department of Energy under Grant number DE-FG02-03ER41270 is gratefully acknowledged.

- Microscopic calculations of in-medium effective NN cross sections in neutron-rich matter [3], a crucial input for the dynamics of heavy-ion collisions. They are also related to other fundamentally important quantities such as the nucleon mean free path and nuclear transparency;
- Isospin-splitting of the mean field in neutron-rich matter [2], also an important component of transport model calculations. Closely related is the isospin splitting of the nucleon effective mass;
- Neutron star properties [4], a most appropriate laboratory to explore the high-density behavior of the EOS.

For a detailed description of previous calculations and results, we refer the reader to our papers already appeared in the literature [1–4]. Here, instead, we will concentrate specifically on our most recent investigations, which address the properties of spin polarized neutron matter. We recall that the study of the magnetic properties of dense matter is of considerable interest in conjunction with the strong magnetic fields existing near the surface of pulsars. The polarizability of nuclear matter can impact the physics of supernovae and proto-neutron stars through, for instance, variations of the neutrino mean free path. As we discuss next, there are fundamentally important and yet unresolved issues concerning the properties of polarized neutron/nuclear matter.

2 Microscopic Calculations of Spin Polarized Neutron Matter

The magnetic properties of neutron/nuclear matter have been studied extensively by many authors and with a variety of theoretical methods (see, for instance, [5–23] for a list that samples the past twenty years). Nevertheless, conclusions about the possibility of a phase transition to a ferromagnetic state at some critical density are still contradictory. For instance, calculations based on Skyrme-type interactions [22] predict that such instabilities will occur with increasing density. In particular, currently used Skyrme forces show a ferromagnetic transition for neutron matter at densities between $1.1\rho_0$ and $3.5\rho_0$ [10]. In fact, spin instability seem to be a common feature among a large class of Skyrme models. In the case of asymmetric matter, calculations with Skyrme effective forces predict a large shift of the critical density for spin instability (towards low densities) even with a very small proton fraction [19]. On the other hand, more recent predictions based on Monte Carlo simulations [13] and the Brueckner-Hartree-Fock (BHF) approach with realistic nucleon-nucleon (NN) interactions [15, 16] exclude these instabilities, at least at densities up to several times normal nuclear density. Relativistic calculations based on effective meson-nucleon Lagrangians [9] predict the ferromagnetic transition to take place at several times nuclear matter density, with its onset being crucially determined by the inclusion of the isovector mesons. Clearly, divergence among predictions concerning the existence of such phase transition is to be found in the different behavior, especially at high density, of the interaction amplitudes describing spin-spin correlations. Thus, this unsettled issue goes to the very core of nuclear physics.

We investigate the bulk and single-particle properties of spin-polarized neutron matter. Our calculation is microscopic and treats the nucleons relativistically. A parameter-free and internally consistent approach makes it easier to interpret the predictions in terms of the underlying nuclear force. This is precisely our focus, namely to understand the in-medium behavior of specific components of the nuclear force (in this case, the spin dependence). Different NN potentials can have comparable quality as seen from their global description of NN data and yet differ in specific features. Thus, it will be interesting to explore how, for a given many-body approach, predictions of ferromagnetic instabilities depend upon specific features of the NN potential. Second, it will be insightful to compare with predictions based on a realistic NN potential and the BHF method [15], especially at the higher densities, where the repulsive Dirac effect can have a dramatic impact on the short-range nature of the force.

The starting point of any microscopic calculation of nuclear structure or reactions is a realistic free-space NN interaction. A realistic and quantitative model for the nuclear force with reasonable theoretical foundations is the one-boson-exchange (OBE) model [24]. Our standard framework consists of the Bonn B potential together with the Dirac-Brueckner-Hartree-Fock (DBHF) approach to nuclear matter. A detailed description of our application of the DBHF method to nuclear, neutron, and asymmetric matter can be found in our earlier works [1, 2, 4].

Similarly to what we have done to describe isospin asymmetries of nuclear matter, the single-particle potential is the solution of a set of coupled equations

$$U_u = U_{ud} + U_{uu} \tag{1}$$

$$U_d = U_{du} + U_{dd} \tag{2}$$

where u and d refer to "up" and "down" polarizations, respectively, and where each $U_{\sigma\sigma'}$ term contains the appropriate (spin-dependent) part of the interaction, $G_{\sigma\sigma'}$. More specifically,

$$U_\sigma(\vec{p}) = \sum_{\sigma'=u,d} \sum_{q\leq k_F^{\sigma'}} < \sigma, \sigma' | G(\vec{p},\vec{q}) | \sigma, \sigma' >, \tag{3}$$

where the second summation indicates integration over the two Fermi seas of spin-up and spin-down neutrons. Clearly, the need to separate the interaction by individual spin components brings along angular dependence, with the result that the single-particle potential depends also on the direction of the momentum.

Solving the G-matrix equation requires knowledge of the single-particle potential, which in turn requires knowledge of the interaction. Hence, Eqs. (1–2) together with the G-matrix equation constitute a self-consistency problem, which is handled, technically, exactly the same way as previously done for the case of isospin asymmetry [1]. Once a self-consistent solution is obtained for the single-particle spectrum, we proceed to calculate the average energy per neutron.

As in the case of isospin asymmetry, it can be expected, and will be verified, that the dependence of the average energy per particle upon the degree of polarization [15] follows the law

$$\bar{e}(\rho,\beta) = \bar{e}(\rho,\beta=0) + S(\rho)\beta^2 \tag{4}$$

where β is the spin asymmetry, defined by $\beta = \dfrac{\rho_u - \rho_d}{\rho}$. A negative value of $S(\rho)$ would signify that a totally polarized system is more stable than unpolarized neutron matter.

From the energy shift,

$$S(\rho) = \bar{e}(\rho,\beta=1) - \bar{e}(\rho,\beta=0), \tag{5}$$

the magnetic susceptibility can be easily calculated. If the parabolic dependence is assumed, then one can write the magnetic susceptibility as [15]

$$\chi = \frac{\mu^2\rho}{2S(\rho)}, \tag{6}$$

where μ is the neutron magnetic moment. The magnetic susceptibility in often expressed in units of χ_F, the magnetic susceptibility of a free Fermi gas,

$$\chi_F = \frac{\mu^2 m}{\hbar^2\pi^2}k_F, \tag{7}$$

where k_F denotes the average Fermi momentum which is related to the total density by

$$k_F = (3\pi^2\rho)^{1/3}. \tag{8}$$

We also recall that the Fermi momenta for up and down neutrons are given by

$$\begin{aligned} k_F^u &= k_F(1+\beta)^{1/3} \\ k_F^d &= k_F(1-\beta)^{1/3}. \end{aligned} \tag{9}$$

3 Results

We begin by showing the angular and momentum dependence of the single-neutron potential, see Figure 1. The angular dependence is generally mild, and becomes more pronounced at the higher momenta. In Figure 2, the asymmetry dependence is displayed for fixed density and momentum (with the angular dependence averaged out). As the density of u particles goes up, the total density remaining constant, the most likely kind of interaction for u neutrons is of the uu type. Similarly, the largest contribution to the d-particle potential is of the du type, see Eqs. (1–2), with the latter being apparently more attractive, as can be inferred by the spin splitting of the potential shown in Figure 2.

The average energy per particle at various densities and as a function of the asymmetry parameter is shown in the third frame of Figure 3. The first two frames display the contribution from the average potential energy and the average kinetic energy, respectively. The parabolic dependence on β, or linear on β^2, is obviously

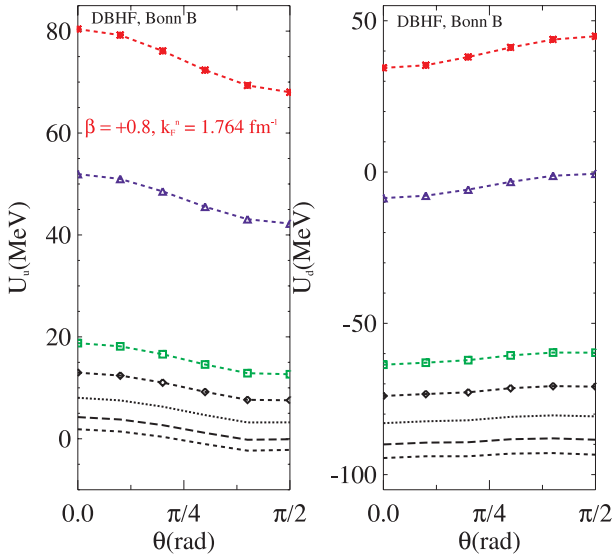

Figure **1.** Angular dependence of the single-particle potential for spin-up and spin-down neutrons at fixed spin asymmetry and Fermi momentum and for different values of the neutron momentum. The momenta are in units of fm^{-1}. The angle is defined relative to the polarization axis.

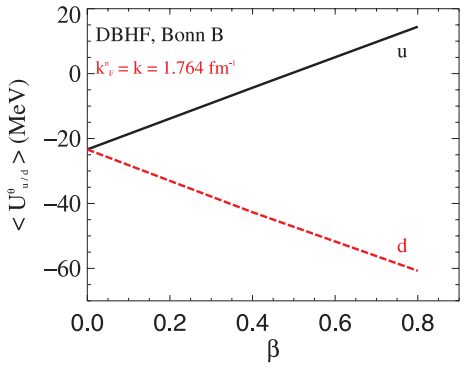

Figure **2.** Asymmetry dependence of the single-particle potential for spin-up and spin-down neutrons at fixed density and momentum. The angular dependence is integrated out.

verified. In Figure 4 we show the corresponding predictions obtained with the conventional Brueckner-Harteee-Fock approach. This comparison may be quite insightful, as we further discuss next. We notice that the Dirac energies are overall more repulsive, but the parabolas predicted with the BHF prescription become steeper as density grows. This is an indication that the energy difference between the totally polarized state and the unpolarized one grows at a faster rate in the non-relativistic calculation. Clearly this is the central issue when predicting the possibility of ferro-

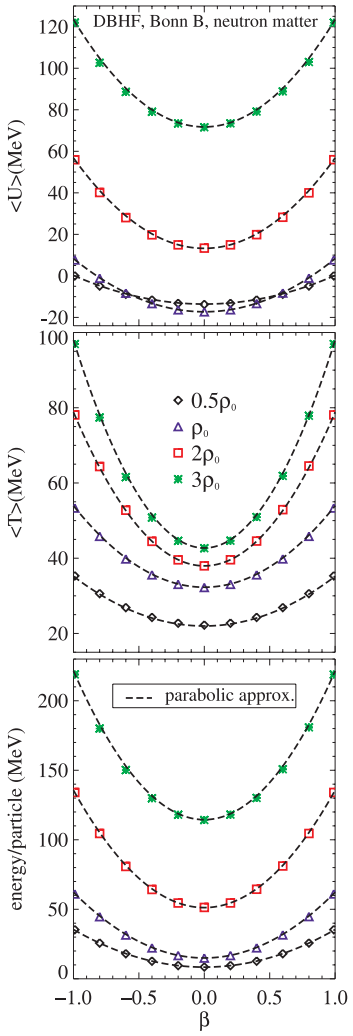

Figure **3.** Average potential, kinetic, and total energy per particle at various densities as a function of the spin asymmetry. Predictions obtained with our standard DBHF calculation.

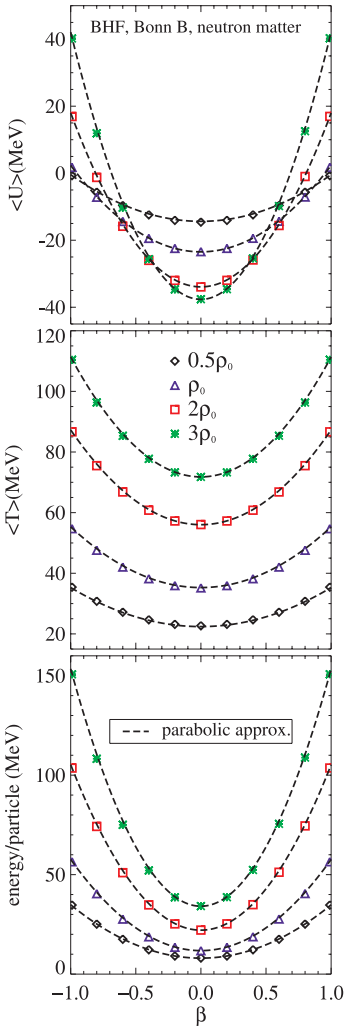

Figure **4.** Same legend as for the previous figure, but the predictions are obtained with the BHF calculation.

magnetic instabilities, which at this point seems more likely to happen in the relativistic model.

This aspect can be revisited through the spin-symmetry energy which we calculate from Eq. (5) and show in Figure 5. Again, for comparison both DBHF and BHF predictions are shown in Figure 5. They confirm the observations made above: although at first the DBHF-based predictions are similar or larger than the BHF ones,

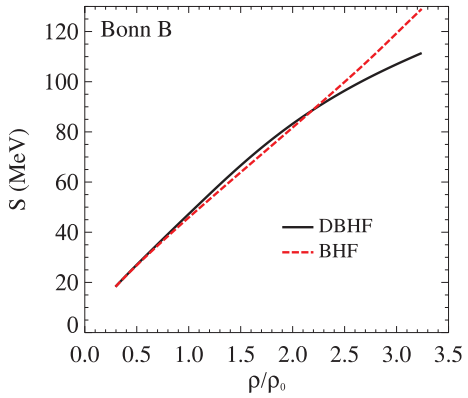

Figure **5.** Density dependence of the spin symmetry energy. Predictions from a conventional Brueckner-Hartree-Fock calculation are also shown.

at high density the energy shift between polarized and unpolarized matter becomes smaller in the relativistic model, although the absolute energies always remain more repulsive in the latter case. A similar observation was already made in conjunction with isospin asymmetry and explained in terms of stronger short-range repulsion in the Dirac model [4]. It must be kept in mind that some large contributions, such as the one from the $^1S_0$ state, are not allowed in the fully polarized case. Now, if such contributions (typically attractive at normal densities) become more and more repulsive with density (due to the increasing importance of short-range repulsive effects), their absence will amount to less repulsive energies at high density. On the other hand, if large and attractive singlet partial waves remain attractive up to high densities, their suppression (demanded in the totally polarized case) will effectively amount to increased repulsion. This is happening in the BHF model, which explains the larger energy shift.

In conclusion, it appears that ferromagnetic instabilities are in principle possible within the Dirac model, although inspection of Figure 5 suggests that very high densities may be necessary for the symmetry energy to turn negative. At that point, softening of the equation of state from additional degrees of freedom not included in the present model may be necessary in order to draw a more definite conclusion. At the present time, however, we can conclude that a Dirac model of nucleons together with (non-strange) mesons has the potential to predict ferromagnetic instabilities, whereas the non-relativistic model shows no indication of such tendency. The latter observation is consistent with previous studies which used the Brueckner-Hartree-Fock approach and the Nijmegen II and Reid93 NN potentials [15]. In fact, comparison with that work allows us to make some useful observations concerning the choice of a particular NN potential, for a similar many-body approach (in this case, BHF). We must keep in mind that off-shell differences exist among NN potentials (even if nearly equivalent in their fit of NN scattering data) and those will impact the G-matrix (which, unlike the T-matrix, is not constrained by the two-body data).

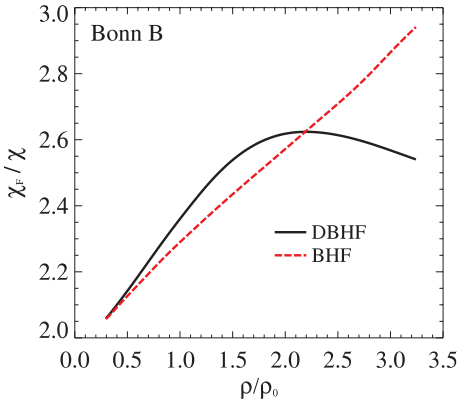

Figure **6.** Density dependence of the ratio χ_F/χ. As in the previous figure, the dashed line is the prediction from a conventional Brueckner-Hartree-Fock calculation.

Furthermore, off-shell differences will have a larger impact at high Fermi momenta, where the higher momentum components of the NN potential, (usually also the most model dependent), play a larger role in the calculation. Accordingly, the best agreement between our BHF predictions and those of [15] is seen at low to moderate densities.

Finally, in Figure 6 we show the ratio χ_F/χ, whose behavior is directly related to the spin-symmetry energy, see Eq. (6). Clearly, similar observations apply to both Figure 5 and Figure 6.

4 Conclusions

We have performed microscopic and self-consistent calculation of the EOS for spin-polarized neutron matter. The EOSs we obtain with the DBHF model are generally rather repulsive at the larger densities. The energy of the unpolarized system (where all nn partial waves are allowed), grows rapidly at high density with the result that the energy difference between totally polarized and unpolarized neutron matter tends to slow down. This may be interpreted as a precursor of spin-separation instabilities. No such tendency is observed in the conventional BHF model. Our calculation, being microscopic and parameter-free, allows us to locate the origin of these model differences in the contributions to the energy from specific partial waves, particularly their behavior in the medium.

In future work, the impact of further extensions will be considered, such as examining the effects of contributions that soften to the EOS (especially at high density), and extending our framework to incorporate both spin- and isospin-asymmetries. It will be interesting to explore whether a crossing of the energies of totally polarized and unpolarized matter occurs at some value of the asymmetry, and what kind of analytical dependence the energy per particle displays as a function of both asymmetry and polarization.

Acknowledgments

Support from the U.S. Department of Energy under grant number DE-FG02-03ER41270 is gratefully acknowledged.

References

1. D. Alonso and F. Sammarruca, *Phys. Rev. C* **67**, 054301 (2003).
2. F. Sammarruca, W. Barredo, and P. Krastev, *Phys. Rev. C* **71**, 064306 (2005).
3. F. Sammarruca and P. Krastev, *Phys. Rev. C* **73**, 014001 (2006).
4. P. Krastev and F. Sammarruca, *Phys. Rev. C* **74**, 025808 (2006).
5. A.D. Jackson, E. Krotscheck, D.E. Meltzer, and R. Smith, *Nucl. Phys. A* **386**, 125 (1982).
6. J. Dabrowski, *Can. J. Phys.* **62**, 400 (1984).
7. A. Vidaurre, J. Navarro, and J. Bernabéu, *Astron. Astrophys.* **135**, 361 (1984).
8. M. Kutshera and W. Wojcik, *Phys. Lett. B* **223**, 11 (1989).
9. S. Marcos, R. Niembro, M.L. Quelle, and J. Navarro, *Phys. Lett. B* **271**, 277 (1991).
10. M. Kutshera and W. Wojcik, *Phys. Lett. B* **325**, 271 (1994).
11. P. Bernardos, S. Marcos, R. Niembro, M.L. Quelle, *Phys. Lett. B* **356**, 175 (1995).
12. V. S. Uma Maheswari, D. N. Basu, J. N. De, and S. K. Samaddar, *Nucl. Phys. A* **615**, 516 (1997).
13. S. Fantoni, A. Sarsa, and K.E. Schmidt, *Phys. Lett.* **87**, 181101 (2001).
14. T. Frick, H. Müther, and A. Sedrakian, *Phys. Rev. C* **65**, 061303 (2002).
15. I. Vidaña, A. Polls, and A. Ramos, *Phys. Rev. C* **65**, 035804 (2002).
16. I. Vidaña and Ignazio Bombaci, *Phys. Rev. C* **66**, 045801 (2002).
17. W. Zuo, U. Lombardo, and C. W. Shen in *Quark-Gluon Plasma and Heavy Ion Collisions*, (ed. W. M. Alberico *et. al.*; World Scientific, Singapore), 192 (2002).
18. W. Zuo, Caiwan Shen, and U. Lombardo, *Phys. Rev. C* **67**, 037301 (2003).
19. A.A. Isayev and J. Yang, *Phys. Rev. C* **69**, 025801 (2004).
20. N. Kaiser, *Phys. Rev. C* **70**, 054001 (2004).
21. Fabio L. Braghin, *Phys. Rev. C* **71**, 064303 (2005).
22. A. Rios, A. Polls, and I. Vidaña, *Phys. Rev. C* **71**, 055802 (2005).
23. I. Bombaci, A. Polls, A. Ramos, A. Rios, and I. Vidaña, *Phys. Lett. B* **632**, 638 (2006).
24. R. Machleidt, *Adv. Nucl. Phys.* **19**, 189 (1989).